論文

モンスーンアジアにおける人為的土地被覆変化による蒸発散量変化の推定

Changes in Evapotranspiration due to Anthropogenic Changes in Land Cover in Monsoon Asia

近藤　昭彦*
Akihiko KONDOH

Abstract: The changes in areal potential evaporation over Monsoon Asia due to land cover changes are estimated by using several global datasets in Global Ecosystem Database version 1.0 CD-ROM (GEDB) by NOAA/EPA.

Cluster analysis is applied to monthly NDVIs in 1990 over Monsoon Asia (60°N-20°S, 60°E-160°E). Forty-eight classes are obtained based on the phenology of the vegetation, and land cover type of each class is determined by warmth index, precipitation and by geographic locations.

Characteristic values of air temperature, cloudiness and seasonal albedos of each class are extracted from GEDB, and areal potential evaporation for current vegetation is calculated using the method of Ahn and Tateishi (1994) based on Priestley and Taylor method.

Natural vegetation of the area of which current land cover is grassland or cropland, is restored by referring Leeman's Holdridge Life Zone dataset. The eastern and southern parts of China and India are subjected to extensive land cover change. Central plains of Myanmar and Thailand are also experienced large land cover change. Areal potential evaporation is calculated for natural vegetation.

論文要旨

NOAA／EPAが作成したGlobal Ecosystem Database version 1.0 CD-ROM(GEDB)に含まれるグローバルデータセットを使用して，モンスーンアジアにおける土地被覆の変化に伴う広域可能蒸発量の変化を推定した。

モンスーンアジアの現植生図を作成するために，NOAA/AVHRRによる1990年の月NDVI(Normalized Difference Vegetation Index)の季節変化に基づき，クラスター分析を行った。48クラスに分類された各クラスごとに気温データから求めることのできる温量指数，降水量の特性を求め，地理的位置を考慮しながら各クラスの植生・土地被覆タイプを決定した。

蒸発量の計算にはPriestley & Taylor法に基づいたAhn and Tateishi(1994)の方法を用いた。計算に必要なパラメーターはGEDBに含まれる気温・日照率・アルベドデータセットを現植生図を重ね合わせ，各クラスの特長値を求めることによって得た。これらのパラメーターを用いて現植生図に対応した広域可能蒸発量を計算した。

自然植生図の復元のために，Holdridge Life Zoneデータセットを参照し，現在草地あるいは農地となっている場所で，気候的には森林が成立可能な地域を抽出した。その結果，計算対象範囲の陸域の約24％の土地被覆が変化していることが推定された。土地被覆の変化面積が大きい地域は中国東部～南部とインドで，タイおよびミャンマーの中央平原がこれに次ぐ。復元された自然植生図に対して現植生図と同じ方法で，可能蒸発量を計算した。

* 筑波大学地球科学系（現千葉大学環境リモートセンシング研究センター）

「写真測量とリモートセンシング」Vol. 34, No. 4, 1995

1. INTRODUCTION

Humans have acquired comfortable life by altering Earth's surface. Recently, many phenomena caused by modification of land cover which make off with pleasant life has appeared successively. Local problems such as heat island of cities, flood in urban area, erosion of cropland, etc., are easy to perceive. The problems over extensive area or that of remote area such as global warming, logging of tropical forest, etc., are hard to experience, but progressing definitely.

Earth's surface has been altered for several thousand years. In Japan, Jomon people (about 8,000 ~300 years B.C.) already cut the trees around their village. Cutting was progressively expanded in Yayoi era (about 300 years B.C.~300 years A.D.) (Yasuda, 1980). Destructions of several civilizations are discussed in connection with disappearance of forests (Yasuda, 1993).

The effects of changes in natural vegetation, mostly forests, for agriculture, human settlements, and other purposes are various. The scientific studies on the effect of forest to hydrological cycle started at the end of nineteenth century in Europe, and great amount of observation records are accumulated. Although the generalization of the results is the theme of future research, it is expected that the runoff is increased and evapotranspiration is decreased by deforestation. As a result, air temperature is considered to be increased to some degree.

In this paper, the author tries to explain "where" and "how much" evapotranspiration has been decreased in Asian region. The one possible way to assess human's impact on regional evapotranspiration is the use of mathematical model which can incorporate the land cover as a model parameter. The accuracy of datasets available and a model applicable, however, is currently incomplete. This paper is an attempt to assess the changes in potential evaporation with land cover changes by using the current available datasets.

2. DATASETS

NOAA/NGDC (National Oceanic and Atmospheric Administration/National Geophysical Data Center) collects the data on the global environment and released as Global Ecosystem Database (GEDB) version 1.0 CD-ROM (Hastings et al., 1992). It contains eighteen global datasets. The most important information when using such a dataset is a document on the production methods and accuracy. GEDB contains the results of reviews by several researchers as well as outline of the datasets and references.

Seven datasets, listed below, are employed from the GEDB. It is easy to point out defects or problems of the datasets, however, the datasets are treated as given data because they are currently the best datasets.

(i) EDC-NESDIS Monthly Experimental Calibrated Global Vegetation Index
(ii) Legates and Willmott Annual Temperature
(iii) Legates and Willmott Annual Corrected Precipitation
(iv) Leemans and Cramer IIASA Mean Monthly Cloudiness
(v) Matthews Seasonal Albedo
(vi) Leeman's Holdridge Life Zone
(vii) Global Elevation and Bathmetry (ETOPO5)

3. CURRENT VEGETATION AND LAND COVER MAP IN ASIA

(1) Classification of Vegetation and Land Cover based on the Seasonal Trend of the Vegetation Index

There are two methods to make a vegetation/land cover map in global or continental scale. The one is to compile existing local vegetation maps. The other is to use satellite remote sensing. The representative of the former method is the Matthews Vegetation Map (Matthews, 1983), which

contained in the GEDB. This method has many problems concerning raw data availability, inconsistency of historical vegetation definitions, a variety of spatial sampling resolutions, and so on. Satellite remote sensing, therefore, is the best way to produce the vegetation map that covers extensive area with high resolution, same accuracy and standardized categories.

EDC-NESDIS Monthly Experimental Calibrated Global Vegetation Index is used to classify land cover in Asia. It is a product of NOAA/AVHRR. The dataset contains the digital number corresponds to NDVI. Original NDVI values are easily restored from the digital number.

The value of NDVI is sometimes smaller than zero. It means that red band reflectance is higher than that of near infrared band, and the signals on vegetation hardly contain in the value. The minus NDVI is replaced by zero, and produce new NDVI dataset.

Investigated area (60°N-20°S, 60°E-160°E) contains Monsoon Asia. Cluster analysis is applied to twelve monthly NDVIs, and forty-eight classes are obtained of which three are meaningless classes due to the effect of mixels.

(2) Interpretation of classes and hydrological functions

Each of the classes is expected to have characteristic hydrological functions. They are the parameters, such as albedo, air temperature, precipitation, etc., necessary for the calculation of hydrological model, and small variance in each class is expected.

Several global datasets are superimposed on the classification map, and the average hydrological functions for each class are extracted. The dataset with different spatial resolution from the NDVI is resampled to make ten minutes grid dataset.

Kira (1945a, b) and Kira et al. (1976) revealed that the distribution of the warmth index is well correspond to the distribution of vegetation formation in Asia. The index is defined as:

$$WI = \Sigma (T_i - 5) \quad i = 1 \text{ to } 12, \ T_i > 5,$$

Table 1 Forest types by Kira's warmth index.

Forest Type	Code	Warmth Index
Tropical Forest	FTR	240<
Subtropical Forest	FST	180—240
Evergreen Broad Leaf Forest	FEB	85—180
Deciduous Broad Leaf Forest	FDB	45— 85
Coniferous Forest	FND	<45

(°C·month)

where Ti is monthly mean air temperatures (℃).

The average indices of each class are calculated from the Legates and Willmott Annual Temperature dataset. Based on the criterion shown in Table 1, current forest type is assigned to each class.

Table 2 shows the statistics of hydrological parameters of each class with standard deviation. If the classification were the one based on the hydrological functions, standard deviation should be small. Unfortunately, it is not so small. Proper classification scheme is the most important subject to be searched for completion of the study.

Fig.1 shows the seasonal patterns of the representative vegetation classes among 45 classes. They have distinctive curves, and it supports the propriety of the classification.

Although it is often difficult to distinguish between a grassland (GRS) and a forest, the category is judged by ΣNDVI and geographic location. The class with ΣNDVI lower than 2.0 is considered as the grassland tentatively.

Because grassland (GRS) and cropland (AGR) are also hard to discriminate, some classes contain both categories. It is decided by geographic location with the use of available atlases. The classes which have bimodal shape in seasonal trend of the NDVI is apparently the land for agriculture as shown in Fig.1.

4. AREAL POTENTIAL EVAPORATION IN MONSOON ASIA

The climatological estimation method is practical to estimate evapotranspiration, because it requires weather elements usually available in the ordinary

Table 2 Results of cluster analysis of monthly NDVIs, and characteristic values of hydrological parameters for each class. Aster (*) means the class that subjects to land cover change in historic era. ΣNDVI:Annual sum of monthly NDVIs, WI : Warmth Index, Pa:Annual Precipitation, Pm : Number of month with Pa>50mm. As for the Leeman's Holdridge Lifezone classes, refer to the document in GEDB or Holdridge (1947, 1967).

No.	Current Class	Restored Class	Leeman's Holdridge	Number of Pixels	(%)	ΣNDVI		WI		Pa		Pm>50mm		
						mean	std.	mean	std.	mean	std.	mean	std.	mode
1	FND	FND	Bor Mois	6124	2.1	2.2	0.1	35.5	12.0	517.5	152.8	4.0	1.8	3
2	DES	DES	ClTmp D/B	1767	0.6	0.2	0.1	114.9	69.9	390.0	733.5	0.0	0.0	0
3	GRS	GRS	Po Des	2250	0.8	1.0	0.2	83.4	64.4	612.4	705.0	2.8	3.0	0
4	GRS	GRS	ClTmp Ste	3928	1.4	1.4	0.2	51.4	25.6	411.8	224.6	2.5	2.0	3
* 5	AGR	FEB	WmTmp DryF	936	0.3	2.6	0.3	126.5	28.7	806.0	437.9	5.1	2.4	3
* 6	GRS/AGR	FND	Bor Mois	4303	1.5	1.9	0.2	38.8	20.7	483.1	185.4	3.5	1.8	3
7	GRS	GRS	ClTmp Ste	3663	1.3	0.9	0.2	70.5	32.7	417.9	331.2	1.6	2.1	0
8	FND	FND	Bor Mois	3050	1.1	2.4	0.2	38.1	15.5	594.4	206.3	5.2	2.4	4
9	AGR	FST	SbTrp MsF	2358	0.8	3.7	0.3	205.5	59.0	1573.1	582.1	6.9	1.7	6
10	GRS	GRS	Po Des	5290	1.8	0.7	0.2	91.6	61.2	522.0	594.2	2.7	2.5	0
11	GRS	GRS	SbTrp ThnS	3176	1.1	1.1	0.2	222.8	61.8	650.3	632.9	3.5	2.0	4
12	FDB	FDB	ClTmp MsF	2819	1.0	3.2	0.3	58.4	15.0	711.7	220.0	5.8	2.2	5
13	FEB	FEB	ClTmp MsF	1900	0.7	3.7	0.3	90.6	28.1	1076.7	454.9	7.9	2.7	7
* 14	AGR	FEB	WmTmp MsF	1462	0.5	2.6	0.3	137.8	44.1	1260.9	489.3	8.4	2.7	11
15	FND	FND	Bor Mois	4734	1.6	2.5	0.2	37.6	12.9	454.3	158.3	3.2	1.7	2
16	FDB	FDB	Bor Mois	3659	1.3	2.7	0.2	52.4	22.7	598.1	233.1	4.6	2.0	5
17	FBS	FBS	Trp VDryF	1888	0.7	2.0	0.3	245.2	48.3	1008.7	710.1	4.9	2.0	5
* 18	GRS	FDB	Bor Mois	2246	0.8	2.0	0.2	54.2	29.9	516.9	259.9	3.7	2.5	3
19	GRS	GRS	ClTmp Ste	3070	1.1	1.5	0.3	70.4	40.8	475.0	426.2	3.1	2.2	2
20	FND	FND	Bor Mois	5304	1.8	2.7	0.2	41.3	8.7	511.3	155.8	4.1	1.7	4
21	GRS	GRS	ClTmp Ste	4436	1.5	2.0	0.2	56.8	27.1	467.1	239.6	3.7	1.7	3
22	FST	FST	SbTrp MsF	1467	0.5	4.3	0.3	212.9	42.4	1795.4	532.9	8.4	1.7	7
23	GRS	GRS	Po Des	8402	2.9	0.4	0.1	104.6	61.9	369.0	510.0	1.4	2.1	0
24	GRS	GRS	Po Rain T	1465	0.5	3.0	0.3	60.0	31.9	663.7	313.9	5.3	1.7	5
25	FTR	FTR	SbTrp WetF	2403	0.8	6.0	0.4	248.6	28.9	2827.6	694.0	11.2	1.6	12
* 26	AGR	FEB	WmTmp DryF	1485	0.5	2.6	0.3	110.7	55.2	937.2	539.0	6.4	2.9	7
* 27	AGR	FTR	Trp DryF	1448	0.5	2.3	0.3	243.4	16.1	920.7	595.0	4.1	2.0	4
* 28	GRS/AGR	FTR	Trp VDryF	1862	0.6	1.5	0.4	246.6	34.9	1108.5	748.5	5.7	1.9	5
* 29	AGR	FEB	WmTmp DryF	979	0.3	3.3	0.3	135.3	30.0	928.8	465.2	6.4	2.1	6
31	FTR	FTR	Trp MsF	1547	0.5	4.3	0.3	242.4	36.0	2343.7	691.3	10.6	2.3	12
32	FTR	FTR	Trp MsF	2289	0.8	5.2	0.3	250.1	23.3	2736.2	653.7	11.2	1.5	12
33	GRS/AGR	GRS/AGR	ClTmp Ste	900	0.3	1.7	0.3	100.1	52.2	616.5	590.8	3.2	3.0	2
34	FEB	FEB	SbTrp MsF	1144	0.4	3.7	0.3	173.3	38.6	1620.1	310.8	9.7	1.5	10
* 35	AGR	FEB	WmTmp MsF	1921	0.7	3.3	0.2	147.0	35.0	1362.0	360.6	9.1	2.1	9
* 36	AGR	FST	SbTrp DryF	663	0.2	3.3	0.4	226.4	22.8	1012.5	646.8	4.7	2.3	4
* 37	GRS/AGR	FTR	SbTrp DryF	1639	0.6	1.9	0.3	246.7	23.2	1103.8	537.5	4.6	1.5	4
* 38	AGR	FTR	SbTrp MsF	1101	0.4	2.9	0.4	246.7	33.6	1678.9	803.4	6.7	1.5	7
* 39	GRS/AGR	FTR	Trp DryF	1440	0.5	3.2	0.3	247.3	34.6	1512.2	729.1	7.0	2.5	6
40	FTR	FTR	SbTrp WetF	2023	0.7	5.2	0.3	250.5	35.5	2740.2	633.2	11.7	1.1	12
* 41	GRS/AGR	FTR	Trp DryF	1654	0.6	2.6	0.3	248.0	22.9	1375.2	466.3	5.5	1.3	5
42	FST	FST	SbTrp MsF	963	0.3	4.3	0.4	238.6	34.9	2323.0	890.9	8.0	1.9	7
43	FST	FST	SbTrp MsF	2237	0.8	4.9	0.3	216.3	40.4	1861.9	635.0	7.9	1.7	8
* 44	AGR	FST	SbTrp MsF	1587	0.6	2.8	0.3	217.3	62.3	1539.0	638.0	7.2	1.7	7
46	FEB	FEB	WmTmp MsF	1193	0.4	4.2	0.3	150.2	56.7	1738.9	582.3	104.4	2.1	12
47	FST	FST	SbTrp MsF	1265	0.4	5.5	0.3	220.0	29.9	2299.6	784.0	8.0	1.0	7

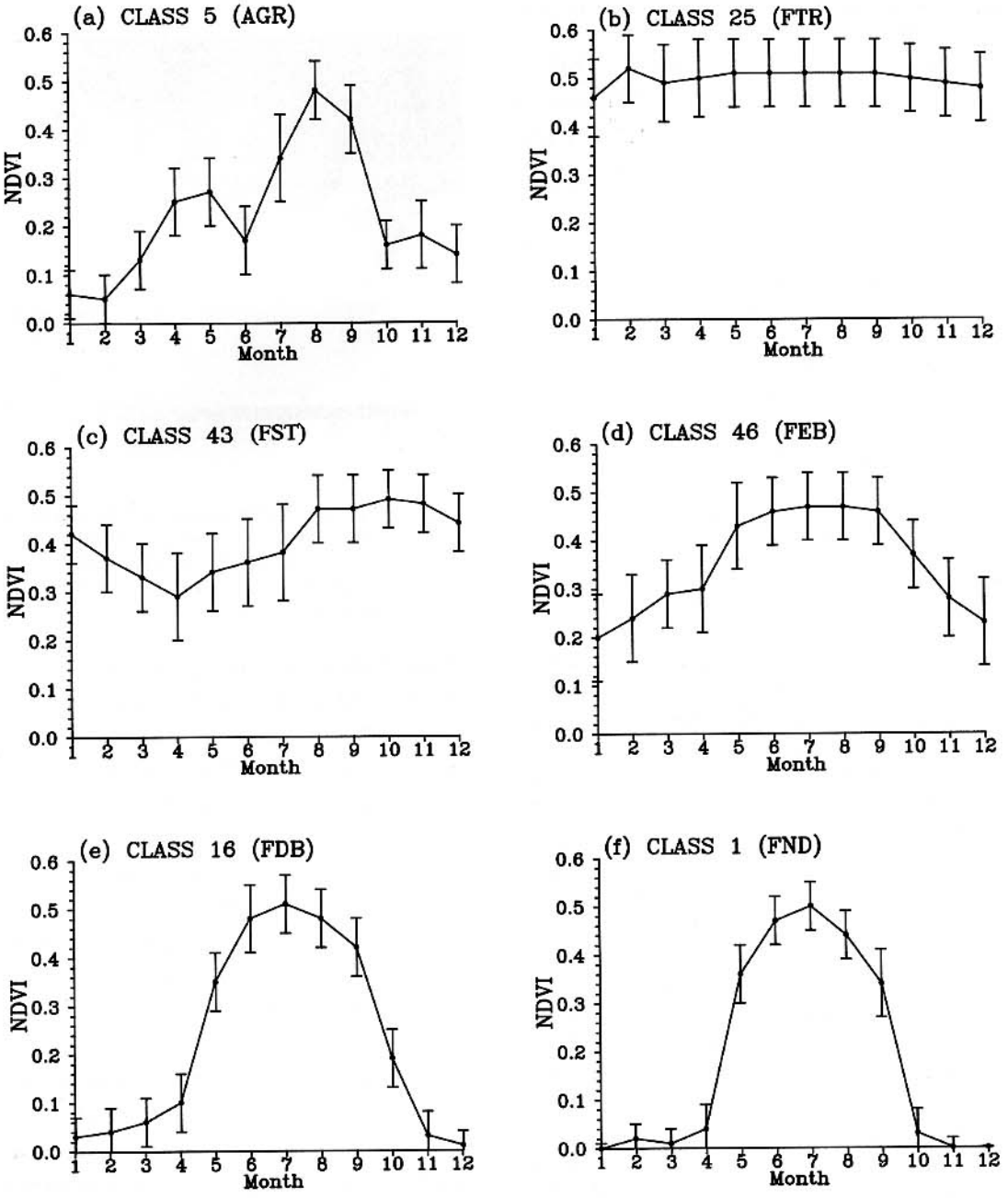

Figure 1 Spectral-temporal plots of selected Asian land cover types. (a) Agriculture fields, (b) Tropical Forest, (c) Sub-tropical forest, (d) Evergreen bloadleaf forest, (e) Deciduous bloadleaf forest, (f) Coniferous forest.

meteorological stations. To estimate the changes in evapotranspiration with the land cover changes, parameters that can be related to land cover should be contained in the algorithm.

Ahn and Tateishi (1994) calculated the global potential evaporation (Ep) by using datasets contained in GEDB. Their method is based on the Priestley and Taylor method (Priestley and Taylor, 1972). It is possible to incorporate the land cover through albedo.

Table 3 Class means of seasonal albedos in percent and standard deviations.

No.	Current Class	Winter		Spring		Summer		Fall	
		mean	std.	mean	std.	mean	std.	mean	std.
1	FND	12.5	1.7	14.7	2.0	17.6	1.5	13.6	1.8
2	DES	24.8	6.3	26.8	6.4	26.4	4.6	25.5	5.5
3	GRS	17.5	5.5	19.9	5.5	21.4	4.5	19.2	5.0
4	GRS	15.9	4.0	18.5	4.3	20.3	3.2	17.8	3.8
5	AGR	14.9	1.1	14.9	3.0	19.3	1.4	16.6	1.3
6	GRS/AGR	13.2	2.2	15.3	2.7	17.9	1.9	14.6	2.5
7	GRS	17.9	5.0	20.4	5.2	22.6	3.9	20.0	4.3
8	FND	13.1	2.1	14.9	2.7	17.4	1.9	14.2	2.1
9	AGR	14.7	3.1	14.9	3.0	15.5	3.2	14.6	2.9
10	GRS	20.0	6.5	22.0	6.0	23.8	4.8	21.7	5.5
11	GRS	20.3	5.9	19.6	6.3	19.5	6.1	19.8	5.9
12	FDB	12.9	2.1	15.0	2.6	17.7	2.2	14.1	2.4
13	FEB	13.2	1.8	15.2	2.2	17.7	2.1	14.5	2.2
14	AGR	14.4	2.7	16.0	3.0	17.4	3.1	15.6	2.9
15	FND	11.5	1.1	13.1	1.8	16.0	1.6	12.6	1.2
16	FDB	13.0	2.0	15.2	2.5	17.8	2.0	14.3	2.4
17	FBS	14.4	4.1	14.6	3.6	15.9	3.6	14.7	3.5
18	GRS	14.9	4.1	17.2	4.4	19.2	3.3	16.4	4.1
19	GRS	17.4	5.1	19.6	4.9	22.1	4.3	19.5	4.6
20	FND	12.2	1.3	14.1	1.6	17.0	1.5	13.2	1.3
21	GRS	16.1	3.9	18.2	3.7	21.2	3.9	18.2	3.8
22	FST	14.0	2.9	14.3	2.7	15.0	3.0	14.2	2.7
23	GRS	22.7	6.7	24.7	6.8	25.1	4.8	23.7	5.8
24	GRS	15.6	3.9	17.9	4.0	19.2	3.5	16.9	4.0
25	FTR	11.7	1.9	11.6	1.6	11.7	1.7	11.6	1.5
26	AGR	13.8	2.9	15.5	3.1	17.4	3.1	15.0	3.0
27	AGR	17.2	2.4	18.1	2.7	19.0	2.7	17.9	2.5
28	GRS/AGR	16.7	2.9	18.2	3.4	19.1	3.3	17.7	3.1
29	AGR	14.8	1.4	17.0	1.4	19.1	1.6	16.4	1.6
31	FTR	12.5	2.8	12.5	2.4	12.6	2.5	12.4	2.4
32	FTR	12.2	2.4	12.1	2.1	12.3	2.4	12.1	2.1
33	GRS/AGR	20.7	6.6	22.8	6.7	23.0	5.1	21.7	5.9
34	FEB	13.5	2.1	14.5	2.3	15.6	2.6	14.4	2.2
35	AGR	13.6	1.8	15.0	2.3	16.5	2.8	14.7	2.3
36	AGR	16.6	2.1	18.1	2.6	19.0	2.9	17.5	2.4
37	GRS/AGR	16.8	1.9	17.4	2.1	18.2	2.5	17.3	1.9
38	AGR	16.3	3.2	17.1	3.9	17.7	3.8	16.8	3.3
39	GRS/AGR	13.7	3.2	13.9	2.6	14.7	2.8	13.9	2.6
40	FTR	11.6	1.5	11.7	1.6	11.8	2.0	11.6	1.5
41	GRS/AGR	16.7	2.0	16.7	2.0	17.1	2.7	16.7	1.9
42	FST	13.3	2.9	13.3	2.8	13.6	3.1	13.2	2.7
43	FST	13.2	2.9	13.2	2.5	13.5	2.9	13.1	2.5
44	AGR	15.2	2.9	16.1	3.0	17.1	3.3	15.9	3.0
46	FEB	13.0	2.1	14.2	2.5	15.5	3.1	13.7	2.4
47	FST	13.0	2.9	12.7	2.4	12.6	2.4	12.7	2.4

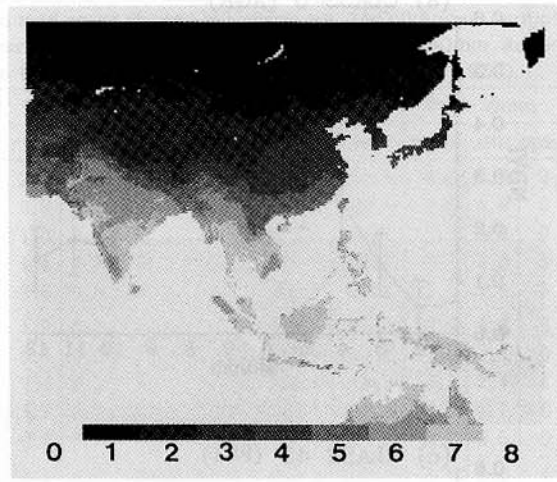

Figure 2 Annual potential evaporation for current vegetation cover. 0: Ocean, 1 : 0-400, 2 : 400-600, 3 : 600-800, 4 : 800-1000, 5 : 1000-1200, 6 : 1200-1400, 7 : 1400-1600, 8 : 1600-(mm/year)

Table 3 shows the class means of seasonal albedos from Matthews Seasonal Albedo dataset in the GEDB. Winter albedo is assigned from December to February, spring albedo from March to May, summer albedo from June to August and autumn albedo from September to November.

Monthly potential evaporations (Ep) are calculated by the method of Ahn and Tateishi (1994) with mean albedo of each land cover (table 3). Another input parameters are extracted from GEDB. As for the details of the method, refer to Ahn and Tateishi (1994).

Fig.2 shows annual Ep in Monsoon Asia for current vegetation cover. The contour of 800 mm/year crosses central Japan. The order of the evapotranspiration seems appropriate in the mid latitudes. Maximum evaporation is in the range between 1600 and 1800 mm/year near equator. The estimates in the humid tropics also seem proper according to the criteria of maximum evapotranspiration in the tropics (Kayane, 1989 ; Kondoh, 1994). It is obvious that Ep overestimates actual evapotranspiration in the semi-arid and arid areas.

Table 4 Average seasonal albedos in percent. N denotes the number of classes to make average.

Class	N	SPRING	SUMMER	FALL	WINTER
FND	9	14.6	17.2	13.8	12.7
FDB	5	15.5	17.7	14.7	13.4
FEB	1	14.2	15.7	13.8	12.8
FST	3	13.0	13.6	12.9	12.8
FTR	2	10.6	10.7	10.6	10.6

(%)

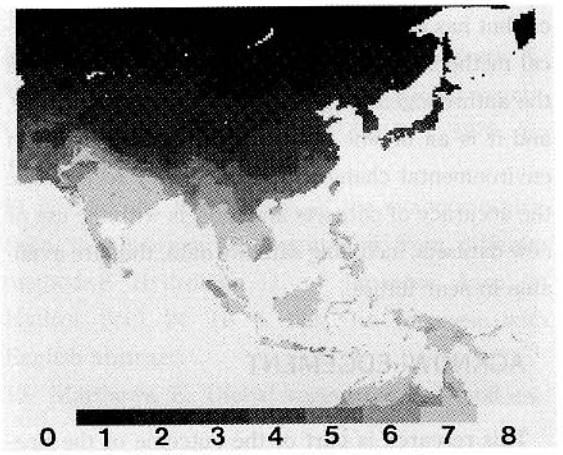

Figure 3 Annual potential evaporation for natural vegetation cover. 0 : Ocean, 1 : 0-400, 2 : 400-600, 3 : 600-800, 4 : 800-1000, 5 : 1000-1200, 6 : 1200-1400, 7 : 1400-1600, 8 : 1600-(mm/year)

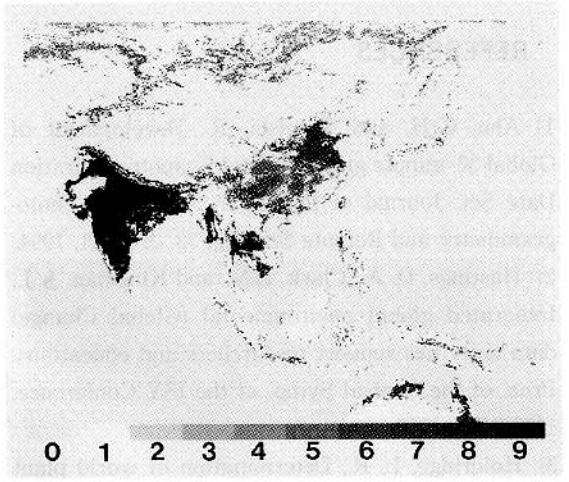

Figure 4 Changes in annual potential evaporation due to land cover changes. 0 : Ocean, 1 : no change, 2 : 0-2, 3 : 2-4, 4 : 4-8, 5 : 8-16, 6 : 16-32, 7 : 32-64, 8 : 64-128, 9 : 128-(mm/year)

5. CHANGES IN LAND COVER AND POTENTIAL EVAPORATION IN MONSOON ASIA

Table 2 contains the classes of Leeman's Holdridge Life Zone (LHLZ) dataset, which means possible vegetation formations under given climatic conditions. It is obtained as the most frequent LHLZ class within a land cover classification class. The classes with aster (*) mean that current vegetation/land cover is grassland or cropland, but climatic condition allows the existence of the forest. Namely, the areas of these classes are subject to change in land cover by humans' activity in the historic era.

These classes account for about 24 per cent of the land area within the calculated region. Most of which occupies India and China. Central plains of Myanmar and Thailand are also experienced large land cover changes.

Natural vegetation is restored based on the warmth index, shown in Table 1. Table 2 contains the restored forest classes. Average seasonal albedo of each forest class is determined as an average of the same class in Table 2. Table 4 shows the average seasonal albedos of the current forest classes. These albedos are assigned to the restored classes, and Ep is recalculated with the same method as Fig. 2.

Fig.3 shows Ep for natural vegetation over Monsoon Asia. Fig.4 shows the amount of changes in Ep between natural and current vegetation.

The region which subject to large areal change in Ep is India and eastern and southern China. Central plain of Myanmar and Thailand is the largest affected area next to India and China. The amount of change is large in India, Myanmar and Thailand.

In China, amount of change in Ep is large in the lower reaches of Hwang Ho River and Yangtze River where the population density is the largest in China. Current land covers of these areas are extensive cropland or paddy field.

The areas that subject to land cover change and the amount of change in evapotranspiration are

both large in Indian Peninsula. It is important that current climatic condition of Decan plateau, central part of the Indian peninsula, is semi-arid when considering the effect of reduction of evapotranspiration.

6. CONCLUDING REMARKS

There are three major problems, they are, (1) the accuracy of the global datasets, (2) the accuracy of the models, and (3) the accuracy of the recognition on the hydrological phenomena. This paper is a trial study on the methodology. The discussion on the absolute value of the evapotranspiration estimates is difficult due to these problems currently unresolved. Followings are the comments for these problems.

Among the global datasets, land cover map is crucial for distributed hydrological modeling. Several international projects are progressing to make high resolution global land cover map with the use of satellite data. In the hydrological viewpoints, it is important to search proper definition of existing land cover that minimizes the variance of hydrological parameters within a class. In other words, it is desirable that a number of hydrological parameters can be derived from the land cover definition for use in the flux calculations. It is the significant subject that must be resolved at an early date.

Regarding the second problem, many sophisticated models are appeared in recent days (for example, Shukla et al., 1990). The accuracy of the results, however, depends on that of input data. It is important before applying the model to know that "what" and "how much" exists "where" in the world, and "what" is the hydrological function of which.

The most important problem is concerning the accuracy of recognition of the phenomena. The results presented in this paper are based on the static model, which could not include the dynamic behavior between vegetation and climate. Many field investigations, that appear in the journals, reveal that there are many factors that must be considered in the model. For example, energy advection, plant growth stage, degree of soil conservation, etc., can influence the water balance at the ground surface.

It is possible to state further difficulties concerning the method adopted in this paper. The model that assigns the hydrological functions to land cover categories and perform static calculations, is practical but has much room to examine. Such an empirical method, however, is one possible way to assess the anthropogenic change in global water balance, and it is an urgent theme in the context of Earth environmental changes. It is necessary to improve the accuracy of datasets and models with the use of new datasets, including satellite data, that are available in near future.

ACKNOWLEDGEMENT

This research is part of the outcome of the Special Research Project on Global Environmental Change at the University of Tsukuba. I appreciate producers and editors of Global Ecosystem Database version 1.0 CD-ROM.

(受付日1995.2.23, 受理日1995.7.11)

REFERENCES

1) Ahn, C-H. and Tateishi, R., Development of Global 30-minute grid Potential Evapotranspiration Date Set. Journal of the Japan Society of Photogrammetry and Remote Sensing, 33, 2, 12-21, 1994.

2) Hastings, D. A., Clark, D.M. and Kineman, J. J., Integrated global environmental (Global Change) data activities support researchers and educations. Proc. of the Central Symp. of the ISY Conference, 1379-1382, 1992.

3) Holdridge, L. R., Determination of world plant formations from simple climatic data. Science, 105, 367-368, 1947.

4) Holdrifge, L.R., Life Zone Ecology. Tropical Science Center, San Jose, 1967. (quoted from

Leemans, 1990).
5) Kayane, I., Water and Meteolorogy. Modern meteorological Technorogy, Vol.1, Asakura-shoten, 272p, 1989. (in Japanese)6) Kira, T., New climatic zonation in eastern Asia as a basis of agricultural geography. Kyoto Imperial University, 24p, 1945a. (in Japanese)
7) Kira, T., New Climatic zonation in southeastern Asia. Kyoto Imperial University, 24p, 1945b. (in Japanese)
8) Kira, T., Shidei, T., Numata, M. and Yoda, K., Vegetation in Japan-Situation in a global vegetation-. Iwanami Kagaku, 46, 235-247, 1976. (in Japanese)
9) Kondoh, A., Comparison of the evapotranspirations in Monsoon Asia estimated from different methods.E Hydrology (J. of Japanese Asoc. of Hydrol. Sci.), 24, 11-30, 1994. (in Japanese with English abstract)
10) Matthews, E., Global vegetation and land use: New high resolution data base for climate studies. J. Clim. Appl. Meteor., 22, 474-487, 1983.
11) NOAA-EPA Global Ecosystem Database Project, Global Ecosystem Database version 1.0, user's guide documentation, reprints and digital data on CD-ROM, USDOC/NOAA National Geophysical Data Center, Boulder, CO., 1992.
12) Priestley, C.H.B. and Taylor, R.J., On the assessment of surface heat flux and evaporation using large-scale parameters. Monthly Weather Review, 100, 81-92, 1972.
13) Shukla, J., Nobre, C. and Sellers, P.J., Amazon deforestation and climatic change. Science, 247, 1322-1325, 1990.
14) Yasuda, Y., The initiation of environmental archeology(環境考古学事始). NHK Books, 365, 270p, 1980. (in Japanese)
15) Yasuda, Y., Climete changes civilization(気候が文明を変える). Iwanami-shoten, 116p, 1993. (in Japanese)